
Boosting Graph Neural Networks by Injecting Pooling in Message Passing

Hyekjin Kwon, Jong-Min Lee
 Hanyang University, Republic of Korea
 {kweon186, 1jm}@hanyang.ac.kr

Abstract

There has been tremendous success in the field of graph neural networks (GNNs) as a result of the development of the message-passing (MP) layer, which updates the representation of a node by combining it with its neighbors to address variable-size and unordered graphs. Despite the fruitful progress of MP GNNs, their performance can suffer from over-smoothing, when node representations become too similar and even indistinguishable from one another. Furthermore, it has been reported that intrinsic graph structures are smoothed out as the GNN layer increases. Inspired by the edge-preserving bilateral filters used in image processing, we propose a new, adaptable, and powerful MP framework to prevent over-smoothing. Our *bilateral*-MP estimates a pairwise modular gradient by utilizing the class information of nodes, and further preserves the global graph structure by using the gradient when the aggregating function is applied. Our proposed scheme can be generalized to all ordinary MP GNNs. Experiments on five medium-size benchmark datasets using four state-of-the-art MP GNNs indicate that the *bilateral*-MP improves performance by alleviating over-smoothing. By inspecting quantitative measurements, we additionally validate the effectiveness of the proposed mechanism in preventing the over-smoothing issue.

1 Introduction

Unlike regular data structures such as images and language sequences, graphs are frequently used to model data with arbitrary topology in many fields of science and engineering [22, 26, 33]. Graph neural networks (GNNs) are promising methods that are used for major graph representation tasks including graph classification, edge prediction, and node classification [9, 15, 18]. In recent years, the most widely used methods for GNNs have learnt node representations by gradually aggregating local neighbors. This is known as message-passing (MP) [10, 11, 17, 29].

Although MP GNNs have proven to be successful in various fields, it has been reported that MP makes node representations closer, leading them to inevitably converge to indistinguishable values with the increase in network depth [35, 37]. This issue, called over-smoothing, impedes the MP GNNs by making all nodes unrelated to the input features and further hurts prediction performance by preventing the model from going deeper [18, 21]. The main cause of over-smoothing is the over-mixing of helpful interaction messages and noise from other node pairs belonging to different classes [7, 37]. Recently, several methods have been developed to alleviate over-smoothing through various normalization schemes, including batch [10, 12], pair [35], and group normalization [37], as well as message reduction via dropping a subset of edges [27] or nodes [7]. However, these methods do not directly consider the fundamental problems of MP GNNs.

In the context of computer vision tasks, some studies may provide insights into this issue. Intuitively, the MP operation can be considered analogous to image filtering, which uses a spatial kernel to extract the weighted sum of values from local neighbors (e.g., mean filter and median filter). The concept

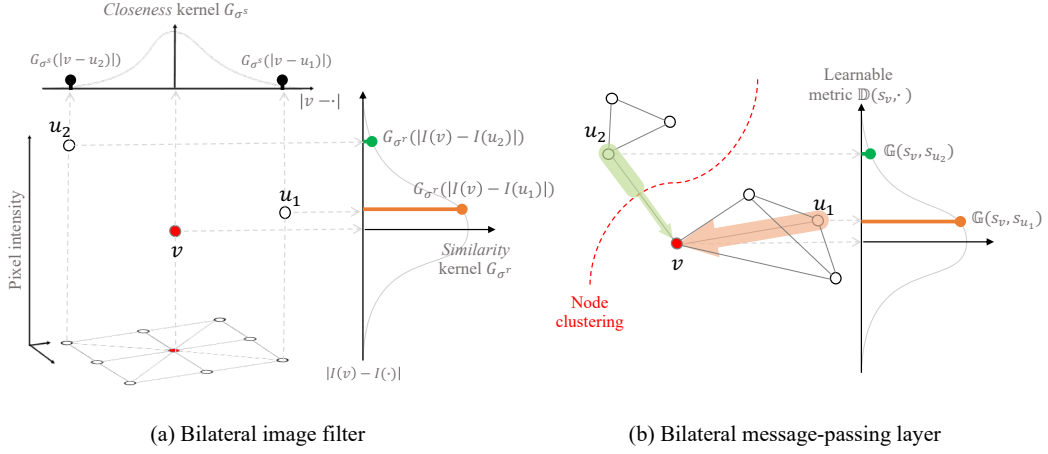


Figure 1: Comparison between (a) the bilateral image filter and (b) proposed *bilateral-MP* layer. The white and red circles denote a set of neighborhood nodes ($u \in \mathcal{N}_v$) and a center node (v), respectively. The bilateral image filter smooths the target image while preserving the edge structure by utilizing the gradient of intensity information $I(\cdot)$ of adjacent pixels (nodes): $I_{bi}(v) = \frac{1}{N} \sum_{u \in V} \mathbb{G}_{\sigma^s}(|v - u|) \mathbb{G}_{\sigma^r}(|I(v) - I(u)|) I(v)$ where \mathbb{G}_{σ^s} is conventional filter kernel of *closeness*, and \mathbb{G}_{σ^r} is regulating kernel of *similarity*. Similarly, given the soft class information s_v for the node v , the proposed *bilateral-MP* layer calculates the modular gradient $\mathbb{G}(s_v, s_u)$, $\forall u \in \mathcal{N}_v$ and regulates the aggregating functions to prevent over-smoothing.

underlying image filtering is slow spatial variation, as adjacent pixels are likely to have similar values [30]. However, this assumption clearly fails at the edges of objects, which serve as boundaries between different homogeneous regions [23]. This poses a challenge for image filtering to preserve local structures. The bilateral filter is a common method that regulates filtering by enforcing not only *closeness* but also *similarity* to prevent over-mixing across edges [30]. The left part of Figure 1 illustrates an example of the bilateral filter. Inspired by this, one may expect a structure-preserving MP mechanism that regulates message aggregation using global information, such as the community structure of the nodes suitable for graphs, to prevent over-smoothing.

Analogous to the bilateral image filter, we propose a new, adaptable, and powerful MP scheme to address over-smoothing in classic MP GNNs. We designed a type of *anisotropic* MP that leverages node classes to estimate the pairwise modular gradient, and further regulates message propagation from neighborhoods using the gradient for better node representation (The right part of Figure 1). Our experiments demonstrate superior performance of the proposed MP scheme over that of most existing diffused GNNs for tasks with the five medium-scale benchmark datasets. To further understand the effect of the proposed *bilateral-MP* scheme, we analyze how the quantitative measurements of over-smoothing change as the number of layers increases. Our work is open-sourced via GitHub, and the code for all models, details for the benchmarking framework, and hyperparameters are available with the PyTorch [25], and DGL [32] frameworks: <https://github.com/hookhy/bi-MP>.

2 Method

In this study, we introduce a new *bilateral-MP* scheme that can be applied to ordinary MP GNN layers to prevent over-smoothing. Instead of directly propagating information through local edges, the proposed model defines a pairwise modular gradient between nodes and uses it to apply a gating mechanism to the MP layer’s aggregating function. More specifically, the *bilateral-MP* takes a soft assignment matrix of as input and extracts the modular gradient by applying metric learning layers to selectively transfer the messages. The key intuition is that the propagation of useful information within the same node class survives while the extraneous noise between different classes is reduced. Thus, the *bilateral-MP* layer results in better graph representation and improved performance by preventing over-smoothing.

2.1 GNNs based on the message-passing

Given a graph $G = (V, E)$ with set of nodes V ($|V| = N$), and edges E , we set the input node feature vectors $\mathbf{x}_v \in \mathbb{R}^{D \times 1}$ for node v , where $\mathbf{X} = [\mathbf{x}_1, \dots, \mathbf{x}_N]^\top$ denotes the feature matrix. Generally, MP GNNs consist of stacked MP layers that learn node representations by applying an update function after aggregating neighboring messages. The update function at layer l is as follows:

$$\mathbf{h}_v^{l+1} = \sigma(\mathbf{U}_1^l \mathbf{h}_v^l + \sum_{u \in \mathcal{N}_v} \mathbf{w}_{u,v} \mathbf{U}_2^l \mathbf{h}_u^l) \quad (1)$$

where \mathcal{N}_v is a set of neighboring nodes, \mathbf{h}_v^l is the feature vector of the node v at layer l , \mathbf{h}_v^0 is set to the input node attribute \mathbf{x}_v , and $\mathbf{U}_1^l \in \mathbb{R}^{D \times D}$, and $\mathbf{U}_2^l \in \mathbb{R}^{D \times D}$ are trainable parameters at layer l . $\mathbf{w}_{u,v}$ is the weighting factor between nodes i and j , and can be scalar or vector (if vector, weighting operation should be performed by applying element-wise multiplication), and σ is the nonlinearity. In the case of *isotropic* MP GNNs, such as Graph Convolutional Networks (GCN) [17] and GraphSAGE [11], $\mathbf{w}_{u,v}$ can be treated as a scalar with a value of 1.

GNNs perform downstream tasks, including node classification, edge prediction, and graph-level prediction, by using additional task-specific layers. First, the task of node classification involves predicting the node label \mathbf{y}_v of the input graph by utilizing the following linear layer:

$$\mathbf{y}_v = \sigma(\mathbf{W}_{\text{FC}} \mathbf{h}_v^L) \quad (2)$$

where $\mathbf{W}_{\text{FC}} \in \mathbb{R}^{C \times D}$ is a trainable parameter with C classes of node labels, and \mathbf{h}_v^L is the final node representation of the last MP layer. To predict the edge attributes \mathbf{y}_e , we can apply a linear layer to the concatenation of the source's representations and determine the edge. We can also perform graph-level prediction by making the linear layer receive the summary vector \mathbf{z}_G for the input graph G . This summary vector \mathbf{z}_G can be obtained by applying the readout-layer, which uses arithmetic operators such as summation and averaging [6].

$$\mathbf{y}_e = \sigma(\mathbf{W}_{\text{FC}} \text{Concat}(\mathbf{h}_{\text{src}}^L, \mathbf{h}_{\text{dst}}^L)), \text{ and } \mathbf{y}_G = \sigma(\mathbf{W}_{\text{FC}} \mathbf{z}_G) \quad (3)$$

In this study, we use the mean readout function for the output representation as follows:

$$\mathbf{z}_G = \frac{1}{N} \sum_{v \in V} \mathbf{h}_v^L \quad (4)$$

2.2 Modular gradient

To circumvent the over-smoothing issue, we intend to reduce the number of incoming messages from the nodes of different classes. This goal suggests the need for the simultaneous definition of 1) node class assignment and 2) measurement of the pairwise difference based on the class information.

By following the node clustering strategy introduced in [37], we train a stack of linear layers using both supervised task-specific loss \mathcal{L}_s and unsupervised loss \mathcal{L}_u based on the minimum cut objective to obtain the node-level class assignment matrix [3]:

$$\mathbf{S}^l = \text{softmax}(\text{ReLU}(\mathbf{H}^l \mathbf{W}_1^l) \mathbf{W}_2^l) \quad (5)$$

$$\mathcal{L}_u = \frac{1}{L} \sum_l \mathcal{L}_u^l \quad (6)$$

where $\mathbf{W}_1^l \in \mathbb{R}^{D \times D}$, and $\mathbf{W}_2^l \in \mathbb{R}^{D \times K^l}$ are trainable parameters, and $\mathbf{H}^l = [\mathbf{h}_1^l, \dots, \mathbf{h}_N^l]^\top$ is the matrix of the hidden representations. For each layer l , the unsupervised loss \mathcal{L}_u^l consists of a spectral

clustering loss \mathcal{L}_c^l based on the k-normalized minimum cut, and an orthogonal loss \mathcal{L}_o^l enabling unique assignment in terms of the node:

$$\mathcal{L}_u^l = \mathcal{L}_c^l + \mathcal{L}_o^l = -\frac{\text{Tr}((\mathbf{S}^l)^\top \tilde{\mathbf{A}} \mathbf{S}^l)}{\text{Tr}((\mathbf{S}^l)^\top \tilde{\mathbf{D}} \mathbf{S}^l)} + \left\| \frac{(\mathbf{S}^l)^\top \mathbf{S}^l}{\|(\mathbf{S}^l)^\top \mathbf{S}^l\|_F} - \frac{\mathbf{I}_K}{\sqrt{K}} \right\|_F \quad (7)$$

where $\text{Tr}(\cdot)$ is a trace operator and $\|\cdot\|_F$ is the Frobenius norm of the matrix. The spectral clustering loss \mathcal{L}_c^l ensures that connected nodes are grouped into the same cluster while partitioning the nodes in K^l disjoint subsets. Minimizing the orthogonal loss \mathcal{L}_o^l enables the cluster assignment vectors $\mathbf{s}_v^l \in \mathbb{R}^{K^l \times 1}, \forall v = 1, \dots, N$ to be orthogonal.

To fulfill the second goal, we propose a novel metric called the modular gradient, which quantifies the pairwise difference of class assignment among the nodes. Specifically, we employ the metric learning mechanism to estimate the generalized Mahalanobis distance $\beta_{u,v}^l$ between the soft cluster assign vectors for the pairs of nodes u , and v as follows [22]:

$$\beta_{u,v}^l = \exp\left(\frac{-\mathbb{D}(\mathbf{s}_u^l, \mathbf{s}_v^l)}{2\sigma_m^2}\right) \quad (8)$$

where $\exp(\cdot)$ denotes an exponential. The sensitivity to the class information of the message passing can be controlled by the hyperparameter σ_m . The Mahalanobis distance kernel $\mathbb{D}(\cdot)$ is defined as:

$$\mathbb{D}(\mathbf{s}_u^l, \mathbf{s}_v^l) = \sqrt{(\mathbf{s}_u^l - \mathbf{s}_v^l)^\top \mathbf{M}^l (\mathbf{s}_u^l - \mathbf{s}_v^l)}, \text{ where } \mathbf{M}^l = \mathbf{W}_m^l \mathbf{W}_m^{l \top} \quad (9)$$

where $\mathbf{W}_m^l \in \mathbb{R}^{D \times D}$ is a trainable parameter and $\mathbb{D}(\cdot)$ is equal to the Euclidean distance metric when $\mathbf{M}^l = \mathbf{I}$. The modular gradient $\beta_{u,v}^l$ will have a large value when nodes u and v belong to the same class, and the opposite case occurs when their assignments are different.

2.3 Bilateral message-passing

The computed modular gradients were further normalized across all neighbors using following function:

$$\hat{\beta}_{u,v}^l = \frac{\text{sigmoid}(\beta_{u,v}^l)}{\sum_{u \in \mathcal{N}_v} \text{sigmoid}(\beta_{u,v}^l)} \quad (10)$$

where $\text{sigmoid}(\cdot)$ is a sigmoid function. Subsequently, we employed a new MP scheme, the *bilateral*-MP, by applying an additional gating mechanism using node class information to the MP layers of Equation 1.

$$\mathbf{h}_v^{l+1} = \sigma(\mathbf{U}_1^l \mathbf{h}_v^l + \sum_{u \in \mathcal{N}_v} \hat{\beta}_{u,v}^l \mathbf{w}_{u,v} \mathbf{U}_2^l \mathbf{h}_u^l) \quad (11)$$

All existing MP GNNs can be improved with the *bilateral*-MP layer(s) by modulating the original layer with a modular gradient as they address the overmixing of harmful noise between different classes.

3 Experiments

In this section, we perform three fundamental supervised graph learning tasks (graph prediction, node classification, and edge prediction) using five medium-size benchmark datasets from diverse domains to evaluate the effectiveness and robustness of the proposed framework. With a unified and reproducible framework of [10], we cover four state-of-the-art (SOTA) MP GNNs: GCN, GraphSAGE, Graph Attention Networks (GAT) [31], and Gated GCN [5]. We also use the quantitative measurement for over-smoothing based on information theory to investigate how the measurement changes by applying the proposed framework.

Table 1: Statistics on five medium-size benchmark datasets. Columns 4 and 5 denote mean statistics for the number of nodes and edges, respectively. Columns 6 and 7 summarize the node and edge features (and dimension), respectively.

Task	Dataset	#Graphs	#Nodes	#Edges	Node feat (dim)	Edge feat (dim)
Graph regression	ZINC	12k	23.16	49.83	Atom type (28)	Bond type (4)
Graph classification	SMNIST	70k	70.57	564.53	intensity+Coordinates (3)	Distance (1)
Graph classification	CIFAR10	60k	117.63	941.07	RGB+Coordinates (5)	Distance (1)
Edge prediction	TSP	12k	275.76	6894.04	Coordinates (2)	Distance (1)
Node classification	CLUSTER	12k	117.20	4301.72	Attributes (7)	—

3.1 Dataset

Following [10], we used two artificially generated (TSP [14], and CLUSTER [1]) and three real-world datasets (SMINIST [20], CIFAR10 [19], and ZINC [13]) with various sizes and complexities, covering all graph tasks. For the graph regression task, we predicted the constrained solubility of the molecular graphs that were randomly selected from the ZINC dataset. We also used the super-pixel datasets SMNIST and CIFAR10, which were converted into a graph classification task using the super-pixels algorithm [2]. The Traveling Salesman problem, which the TSP dataset is based in, is one of the most intensively studied problems relating to the multiscale and complex nature of 2D Euclidean graphs. As shown in [10], we cast the TSP as a binary edge prediction task that identifies the optimal edges given by the Concorde. CLUSTER, a semi-supervised node classification task, was generated using stochastic block models (SBM), which can be used to model community structures [1]. More details for the datasets are presented in [10], and corresponding statistics are reported in Table 1.

3.2 Benchmarking framework

For all datasets, we followed the same benchmarking protocol, which encompasses the method for data splits, pre-processing, performance metrics, and other training details in [10], to ensure a fair comparison. We reported summary statistics (mean, and the standard deviation) of the performance metrics over four runs with different seeds of initialization. We used the same learning rate decay strategy as in [10] to train the models using the Adam optimizer [16]. More details for the implementation of the experiments are provided in the GitHub repository.

3.3 GNN layers and network architecture

We considered two *isotropic* and two *anisotropic* MP GNNs as baselines. We modified these SOTA models by applying the proposed *bilateral*-MP algorithm and compared prediction performance with that of the original models. All GNNs consist of L -MP layers, and details of each SOTA GNN are reported in Appendix A. To apply the *bilateral*-MP layer to the SOTA GNNs, we proposed three variations of network configuration: *boosting*, *interleaved*, and *dense*. The *boosting* configuration only adopts a *bilateral*-MP layer at the initial part, while the other layers are unchanged. Specifically, only the second layer is modified to ensure better conditions for the soft cluster assignment networks in the *bilateral*-MP layer. The *interleaved* configuration alternates between ordinary and *bilateral*-MP layers, and the *dense* configuration consists only of *bilateral*-MP layers. Heuristically, we reported the experimental results using only the *boosting* configuration. The results and details for the other configurations can be found in Appendix B. We used the same setting as in [10] for any possible other basic building blocks, such as batch normalization, residual connection, and dropout. The hyperparameters for the number of layers and dimensions of the hidden and output representations for each layer are defined accordingly to match the parameter budgets proposed in [10]: 100k or 500k parameters. Finally, the task-specific networks which were mentioned in Section 2.1 are applied to the output of the stacked GNN layers, and other details for the implementation can be found in the GitHub repository.

3.4 Benchmarking results

Graph-level predictions. As shown in Table 2, the proposed *bilateral*-MP exhibits consistently high performance across datasets and MP GNNs. All models with the *bilateral*-MP framework

Table 2: Benchmarking results on four SOTA MP GNNs across datasets of graph-level prediction tasks. L and Params denote the number of layers and network parameters, respectively. We reported the statistics for mean absolute error (MAE), and prediction accuracy (ACC). Epochs refers number of epochs for convergence. **Bold**: there are performance improvements with our *bilateral*-MP scheme. **Red**: Best performance.

ZINC									
Model	L	Params	Test MAE	Train MAE	Epochs	Model	L	Params	Test MAE
GraphSAGE	4	103077	0.459 \pm 0.006	0.343 \pm 0.011	196.25	<i>bi</i> -GCN	4	125651	0.394 \pm 0.006
	4	94977	0.468 \pm 0.003	0.251 \pm 0.004	147.25	<i>bi</i> -GraphSAGE	4	115389	0.305 \pm 0.019
	4	102385	0.475 \pm 0.007	0.317 \pm 0.006	137.5	<i>bi</i> -GAT	4	105256	0.410 \pm 0.017
	4	105875	0.375 \pm 0.003	0.236 \pm 0.007	194.75	<i>bi</i> -GatedGCN	4	11574	0.310 \pm 0.038
GatedGCN	16	505079	0.367 \pm 0.011	0.128 \pm 0.019	197	<i>bi</i> -GCN	16	536482	0.276 \pm 0.007
	16	505341	0.398 \pm 0.002	0.081 \pm 0.009	145.5	<i>bi</i> -GraphSAGE	16	516651	0.245 \pm 0.009
	16	531345	0.384 \pm 0.007	0.067 \pm 0.004	144	<i>bi</i> -GAT	16	535536	0.277 \pm 0.012
	16	505011	0.214 \pm 0.013	0.067 \pm 0.019	185	<i>bi</i> -GatedGCN	16	511974	0.166 \pm 0.009
SMNIST									
Model	L	Params	Test ACC	Train ACC	Epochs	Model	L	Params	Test ACC
GCN	4	110807	90.705 \pm 0.218	97.196 \pm 0.223	127.5	<i>bi</i> -GCN	4	104217	90.805 \pm 0.299
	16	505341	97.312 \pm 0.097	100.00 \pm 0.000	98.25	<i>bi</i> -GraphSAGE	4	110400	97.438 \pm 0.155
	4	114169	95.535 \pm 0.205	99.994 \pm 0.008	104.75	<i>bi</i> -GAT	4	104337	95.363 \pm 0.199
	4	114507	97.340 \pm 0.143	100.00 \pm 0.000	96.25	<i>bi</i> -GatedGCN	4	101365	97.515 \pm 0.085
CIFAR10									
Model	L	Params	Test ACC	Train ACC	Epochs	Model	L	Params	Test ACC
GraphSAGE	4	101657	55.710 \pm 0.381	69.523 \pm 1.948	142.5	<i>bi</i> -GCN	4	125564	54.450 \pm 0.137
	4	1104517	65.767 \pm 0.308	99.719 \pm 0.062	93.5	<i>bi</i> -GraphSAGE	4	114312	64.863 \pm 0.445
	4	110704	64.223 \pm 0.455	89.114 \pm 0.499	103.75	<i>bi</i> -GAT	4	114311	64.275 \pm 0.458
	4	104357	67.312 \pm 0.311	94.553 \pm 1.018	97	<i>bi</i> -GatedGCN	4	110632	67.850 \pm 0.522

Table 3: Benchmarking results on four SOTA MP GNNs across datasets of edge- and node-level prediction tasks. We report the statistics for F1 score (F1), and prediction accuracy (ACC). **Bold**: there are performance improvements with our bilateral MP scheme. **Red**: Best performance.

TSP									
Model	L	Params	Test F1	Train F1	Epochs	Model	L	Params	Test F1
GCN	4	95702	0.630 \pm 0.001	0.631 \pm 0.001	261	<i>bi</i> -GCN	4	118496	0.642 \pm 0.001
	4	99263	0.665 \pm 0.003	0.669 \pm 0.003	266	<i>bi</i> -GraphSAGE	4	131861	0.693 \pm 0.016
	4	96182	0.673 \pm 0.002	0.671 \pm 0.002	328.25	<i>bi</i> -GAT	4	115609	0.675 \pm 0.002
	4	97858	0.808 \pm 0.003	0.811 \pm 0.003	197	<i>bi</i> -GatedGCN	4	125832	0.812 \pm 0.004
CLUSTER									
Model	L	Params	Test ACC	Train ACC	Epochs	Model	L	Params	Test ACC
GraphSAGE	16	501687	68.498 \pm 0.976	71.729 \pm 2.212	79.75	<i>bi</i> -GCN	16	505149	71.199 \pm 0.882
	16	503350	63.844 \pm 0.110	86.710 \pm 0.167	57.75	<i>bi</i> -GraphSAGE	16	490569	64.088 \pm 0.182
	16	527824	70.587 \pm 0.447	76.074 \pm 1.362	73.5	<i>bi</i> -GAT	16	445438	71.113 \pm 0.869
	16	504253	76.082 \pm 0.196	88.919 \pm 0.720	57.75	<i>bi</i> -GatedGCN	16	516211	76.896 \pm 0.213

outperform the baseline MP GNNs for the graph-level regression task on the ZINC dataset. Among the MP GNNs, the gated GCN with the *bilateral*-MP (*bi*-gated GCN) yields superior performance to that of other GNNs, including its baseline network (*vanilla* gated GCN). Similarly, the best results in the graph classification task were yielded by the *bi*-gated GCN. Results from the other baseline MP GNNs (GraphSAGE, GAT, and GCN) indicate that the proposed scheme boosts prediction performance, except in the cases of GAT on SMNIST and isotropic models on CIFAR10.

Node- and edge-level predictions. Table 3 reports the results for both the edge prediction and node classification tasks with the TSP and CLUSTER datasets. In the case of TSP, all GNNs using the proposed *bilateral*-MP achieved higher performance than their respective baseline models. Our *bilateral*-MP framework injects global-level information (the node class) in message aggregation to prevent over-localization. Thus, these results were expected because TSP graphs require reasoning about both local- (neighborhood nodes) and global-level (node class information) graph structures. On the CLUSTER dataset, the proposed framework adapts the GNNs to better represent the graphs that are highly modularized using the SBM. As a result, the experiments on CLUSTER also show that the performance of *bilateral*-MP GNNs is consistently better than that of the baseline GNNs. The *bi*-gated GCN achieves the best performance among the models.

Small-size benchmark datasets. In addition to these medium-size benchmarking results, we also performed graph classification tasks using three other small-sized datasets: DD [28], PROTEINS [4], and ENZYME [36]. We reported the details and results of the experiments on small-sized datasets in Appendix C.

3.5 Quantitative feature analysis

In Section 3.4, we demonstrated the robustness and effectiveness of our proposed framework on graph machine-learning tasks. In this section, we performed an additional analysis to understand how the *bilateral-MP* prevents over-smoothing. We quantitatively measured over-smoothing to investigate how it changes along the layers. To eliminate any undesired effect, we adopted the simplest model and its variant: GCN with and without the *boosting bilateral-MP* layer (*bi-GCN*). With the same setting as the above benchmarking experiments, these GNNs were trained and subsequently used to infer the test graphs using the CLUSTER dataset. Given a test graph G , we obtained the instance information gain I_G^l based on the information theory at each layer l [37].

$$I_G^l = \sum_v P_{\mathbf{X}, \mathbf{H}^l}(x_v, h_v) \log \frac{P_{\mathbf{X}, \mathbf{H}^l}(x_v, h_v)}{P_{\mathbf{X}}(x_v) P_{\mathbf{H}^l}(h_v)} \quad (12)$$

where $P_{\mathbf{X}}$, and $P_{\mathbf{H}^l}$ are the probability distributions of the input feature, and the hidden representation at layer l , respectively, both defined under the Gaussian assumption. $P_{\mathbf{X}, \mathbf{H}^l}$ denotes joint distribution. The instance information gain is a measurement of the mutual information between the input feature and hidden representation. Thus, the values of I_G^l tend to decrease with the intensification of over-smoothing, as node embeddings lose their input information by averaging neighbor information. As shown in Figure 3, the information gains of the proposed model are significantly higher than those of the baseline model along the layers. This result suggests that our *bilateral-MP* framework can prevent the over-smoothing issue.

4 Conclusion

In this study, we introduced a new *bilateral-MP* scheme to minimize over-smoothing. To prevent over-mixing of node representations across different classes, the proposed model regulates the aggregating layer by utilizing the global community structure with the class information of nodes. Our model boosts the performance of existing GNNs by preventing over-smoothing. We expect to contribute to the community by providing a simple insight and sanity-check for novel MP GNNs in the future.

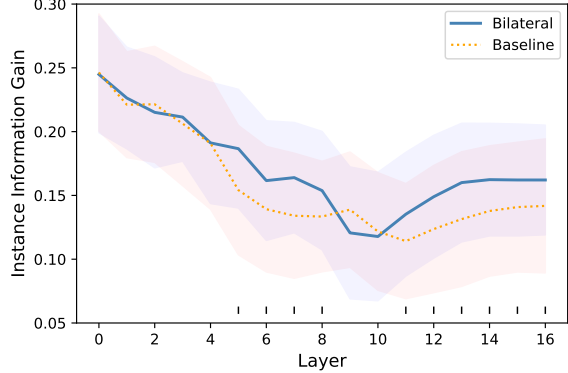


Figure 2: Comparison of the instance information gain between *bi-GCN* and *vanilla GCN* across the layers. The solid (and dashed) lines and shaded region denote mean and standard deviation for the $1k$ test graphs of CLUSTER, respectively. Short vertical bars indicate a statistically significant difference in the two-sampled T-tests between the baseline and proposed models after Bonferroni multiple-comparison correction.

Acknowledgments and Disclosure of Funding

This work was supported by Institute of Information & communications Technology Planning & Evaluation (IITP) grant funded by the Korea government(MSIT) (No.2020-0-01373, Artificial Intelligence Graduate School Program(Hanyang University))

References

- [1] Emmanuel Abbe. Community detection and stochastic block models: recent developments. *The Journal of Machine Learning Research*, 18(1):6446–6531, 2017.
- [2] Radhakrishna Achanta, Appu Shaji, Kevin Smith, Aurelien Lucchi, Pascal Fua, and Sabine Süstrunk. Slic superpixels compared to state-of-the-art superpixel methods. *IEEE transactions on pattern analysis and machine intelligence*, 34(11):2274–2282, 2012.
- [3] Filippo Maria Bianchi, Daniele Grattarola, and Cesare Alippi. Mincut pooling in graph neural networks. *CoRR*, abs/1907.00481, 2019. URL <http://arxiv.org/abs/1907.00481>.
- [4] Karsten M Borgwardt, Cheng Soon Ong, Stefan Schönauer, SVN Vishwanathan, Alex J Smola, and Hans-Peter Kriegel. Protein function prediction via graph kernels. *Bioinformatics*, 21(suppl_1):i47–i56, 2005.
- [5] Xavier Bresson and Thomas Laurent. Residual gated graph convnets. *arXiv preprint arXiv:1711.07553*, 2017.
- [6] Cătălina Cangea, Petar Veličković, Nikola Jovanović, Thomas Kipf, and Pietro Liò. Towards sparse hierarchical graph classifiers. *arXiv preprint arXiv:1811.01287*, 2018.
- [7] Deli Chen, Yankai Lin, Wei Li, Peng Li, Jie Zhou, and Xu Sun. Measuring and relieving the over-smoothing problem for graph neural networks from the topological view, 2019.
- [8] Djork-Arné Clevert, Thomas Unterthiner, and Sepp Hochreiter. Fast and accurate deep network learning by exponential linear units (elus), 2016.
- [9] Gabriele Corso, Luca Cavalleri, Dominique Beaini, Pietro Liò, and Petar Veličković. Principal neighbourhood aggregation for graph nets, 2020.
- [10] Vijay Prakash Dwivedi, Chaitanya K. Joshi, Thomas Laurent, Yoshua Bengio, and Xavier Bresson. Benchmarking graph neural networks, 2020.
- [11] William L. Hamilton, Rex Ying, and Jure Leskovec. Inductive representation learning on large graphs, 2018.
- [12] Sergey Ioffe and Christian Szegedy. Batch normalization: Accelerating deep network training by reducing internal covariate shift, 2015.
- [13] John J Irwin, Teague Sterling, Michael M Mysinger, Erin S Bolstad, and Ryan G Coleman. Zinc: a free tool to discover chemistry for biology. *Journal of chemical information and modeling*, 52(7):1757–1768, 2012.
- [14] Chaitanya K Joshi, Thomas Laurent, and Xavier Bresson. An efficient graph convolutional network technique for the travelling salesman problem. *arXiv preprint arXiv:1906.01227*, 2019.
- [15] Amir Hosein Khasahmadi, Kaveh Hassani, Parsa Moradi, Leo Lee, and Quaid Morris. Memory-based graph networks, 2020.
- [16] Diederik P. Kingma and Jimmy Ba. Adam: A method for stochastic optimization, 2017.
- [17] Thomas N. Kipf and Max Welling. Semi-supervised classification with graph convolutional networks, 2017.
- [18] Johannes Klicpera, Aleksandar Bojchevski, and Stephan Günnemann. Predict then propagate: Graph neural networks meet personalized pagerank, 2019.
- [19] Alex Krizhevsky, Geoffrey Hinton, et al. Learning multiple layers of features from tiny images.(2009), 2009.

[20] Yann LeCun, Léon Bottou, Yoshua Bengio, and Patrick Haffner. Gradient-based learning applied to document recognition. *Proceedings of the IEEE*, 86(11):2278–2324, 1998.

[21] Guohao Li, Matthias Müller, Ali Thabet, and Bernard Ghanem. Deepgcns: Can gcns go as deep as cnns?, 2019.

[22] Ruoyu Li, Sheng Wang, Feiyun Zhu, and Junzhou Huang. Adaptive graph convolutional neural networks, 2018.

[23] Wei Liu, Pingping Zhang, Xiaogang Chen, Chunhua Shen, Xiaolin Huang, and Jie Yang. Embedding bilateral filter in least squares for efficient edge-preserving image smoothing. *IEEE Transactions on Circuits and Systems for Video Technology*, 30(1):23–35, 2018.

[24] Christopher Morris, Nils M Kriege, Franka Bause, Kristian Kersting, Petra Mutzel, and Marion Neumann. Tudataset: A collection of benchmark datasets for learning with graphs. *arXiv preprint arXiv:2007.08663*, 2020.

[25] Adam Paszke, Sam Gross, Francisco Massa, Adam Lerer, James Bradbury, Gregory Chanan, Trevor Killeen, Zeming Lin, Natalia Gimelshein, Luca Antiga, et al. Pytorch: An imperative style, high-performance deep learning library. *Advances in neural information processing systems*, 32:8026–8037, 2019.

[26] Ekagra Ranjan, Soumya Sanyal, and Partha Pratim Talukdar. Asap: Adaptive structure aware pooling for learning hierarchical graph representations, 2020.

[27] Yu Rong, Wenbing Huang, Tingyang Xu, and Junzhou Huang. Dropedge: Towards deep graph convolutional networks on node classification, 2020.

[28] Ryan A. Rossi and Nesreen K. Ahmed. The network data repository with interactive graph analytics and visualization. In *AAAI*, 2015. URL <https://networkrepository.com>.

[29] Sainbayar Sukhbaatar, Arthur Szlam, and Rob Fergus. Learning multiagent communication with backpropagation, 2016.

[30] Carlo Tomasi and Roberto Manduchi. Bilateral filtering for gray and color images. In *Sixth international conference on computer vision (IEEE Cat. No. 98CH36271)*, pages 839–846. IEEE, 1998.

[31] Petar Veličković, Guillem Cucurull, Arantxa Casanova, Adriana Romero, Pietro Lio, and Yoshua Bengio. Graph attention networks. *arXiv preprint arXiv:1710.10903*, 2017.

[32] Minjie Wang, Da Zheng, Zihao Ye, Quan Gan, Mufei Li, Xiang Song, Jinjing Zhou, Chao Ma, Lingfan Yu, Yu Gai, Tianjun Xiao, Tong He, George Karypis, Jinyang Li, and Zheng Zhang. Deep graph library: A graph-centric, highly-performant package for graph neural networks. *arXiv preprint arXiv:1909.01315*, 2019.

[33] Zonghan Wu, Shirui Pan, Fengwen Chen, Guodong Long, Chengqi Zhang, and Philip S. Yu. A comprehensive survey on graph neural networks. *IEEE Transactions on Neural Networks and Learning Systems*, 32(1):4–24, Jan 2021. ISSN 2162-2388. doi: 10.1109/tnnls.2020.2978386. URL <http://dx.doi.org/10.1109/TNNLS.2020.2978386>.

[34] Bing Xu, Naiyan Wang, Tianqi Chen, and Mu Li. Empirical evaluation of rectified activations in convolutional network, 2015.

[35] Lingxiao Zhao and Leman Akoglu. Pairnorm: Tackling oversmoothing in gnns, 2020.

[36] Wenting Zhao, Chunyan Xu, Zhen Cui, Tong Zhang, Jiatao Jiang, Zhenyu Zhang, and Jian Yang. When work matters: Transforming classical network structures to graph cnn, 2018.

[37] Kaixiong Zhou, Xiao Huang, Yuening Li, Daochen Zha, Rui Chen, and Xia Hu. Towards deeper graph neural networks with differentiable group normalization, 2020.

Boosting Graph Neural Networks by Injecting Pooling in Message Passing

— Supplementary material —

A Details of the bilateral-GNN layer

In this section, we present details for the SOTA MP layers and their bilateral variants, which were used for the benchmarking experiments in Section 3.4. The MP GNNs, consisting of L -layers that embed the node representations, can consider multi-hop neighborhoods [37].

Graph Convolutional Networks (GCN). GCN layers can be implemented as a simple MP using some approximations and simplifications of the Chebyshev polynomials [17]:

$$\mathbf{h}_v^{l+1} = \text{ReLU}(\mathbf{U}^l \frac{1}{\deg_v} \sum_{u \in \mathcal{N}_v} \mathbf{h}_u^l) \quad (\text{S1})$$

where \deg_v denotes the degree of node v , and $\mathbf{U}^l \in \mathbb{R}^{D \times D}$ is a trainable parameter. We applied modular gradient weighting in Section 2.2 to the aggregating function of Equation S1 to define the *bi*-GCN layer:

$$\mathbf{h}_v^{l+1} = \text{ReLU}(\mathbf{U}^l \frac{\hat{\beta}_{u,v}^l}{\deg_v} \sum_{u \in \mathcal{N}_v} \mathbf{h}_u^l) \quad (\text{S2})$$

GraphSAGE. Following [10], we use the GraphSAGE layer utilizing a max aggregator [11]:

$$\mathbf{h}_v^{l+1} = \text{ReLU}(\mathbf{U}^l \text{Concat}(\mathbf{h}_v^l, \text{Max}_{u \in \mathcal{N}_v} \text{ReLU}(\mathbf{V}^l \mathbf{h}_u^l))) \quad (\text{S3})$$

where $\text{Max}(\cdot)$ is the maxpooling operator, and $\mathbf{U}^l \in \mathbb{R}^{D \times D}$, and $\mathbf{V}^l \in \mathbb{R}^{D \times D}$ are trainable parameters. We applied modular gradient weighting in Section 2.2 to the aggregating function of Equation S3 to define the *bi*-GraphSAGE layer:

$$\mathbf{h}_v^{l+1} = \text{ReLU}(\mathbf{U}^l \text{Concat}(\mathbf{h}_v^l, \text{Max}_{u \in \mathcal{N}_v} \hat{\beta}_{u,v}^l \text{ReLU}(\mathbf{V}^l \mathbf{h}_u^l))) \quad (\text{S4})$$

Graph Attention Networks (GAT). GAT layers embed representation of a center node by applying multi-head self-attention strategy with representations of neighborhood nodes [31]. The pairwise self-attention scores $e_{u,v}^{k,l}$ at layer l and head k were normalized and used to perform *anisotropic* propagation of the neighborhood messages:

$$\mathbf{h}_v^{l+1} = \text{Concat}_{k=1}^K (\text{ELU}(\sum_{u \in \mathcal{N}_v} e_{u,v}^{k,l} \mathbf{U}^{k,l} \mathbf{h}_u^l)) \quad (\text{S5})$$

$$e_{u,v}^{k,l} = \frac{\exp(\hat{e}_{u,v}^{k,l})}{\sum_{u \in \mathcal{N}_v} \exp(\hat{e}_{u,v}^{k,l})} \quad (\text{S6})$$

$$\hat{e}_{u,v}^{k,l} = \text{lReLU}(\mathbf{V}^{k,l} \text{Concat}(\mathbf{U}^{k,l} \mathbf{h}_v^l, \mathbf{U}^{k,l} \mathbf{h}_u^l)) \quad (\text{S7})$$

Table S1: Benchmarking results on gated GCN on the ZINC dataset across three network configurations. **Bold**: there are performance improvements with our *bilateral*-MP scheme. **Red**: Best performance.

Model	L	Params	Test MAE	Train MAE	Epochs	L	Params	Test MAE	Train MAE	Epochs
GatedGCN	4	105875	0.375 ± 0.003	0.236 ± 0.007	194.75	16	505011	0.214 ± 0.013	0.067 ± 0.019	185
<i>boosting</i> -GatedGCN	4	111574	0.310 ± 0.038	0.186 ± 0.060	208.5	16	511974	0.166 ± 0.009	0.049 ± 0.015	212.75
<i>interleaved</i> -GatedGCN	4	117273	0.372 ± 0.011	0.220 ± 0.028	180.75	16	560715	0.213 ± 0.012	0.073 ± 0.005	192.75
<i>dense</i> -GatedGCN	4	128671	0.369 ± 0.025	0.204 ± 0.031	205	16	616419	0.210 ± 0.013	0.064 ± 0.012	189.75

where ELU and IReLU denote the exponential linear unit (ELU) [8], and leaky ReLU nonlinearity [34] functions, respectively. We applied modular gradient weighting in Section 2.2 to the aggregating function of Equation S5 to define the *bi*-GAT layer:

$$\mathbf{h}_v^{l+1} = \text{Concat}_{k=1}^K (\text{ELU}(\sum_{u \in \mathcal{N}_v} \hat{\beta}_{u,v}^l e_{u,v}^{k,l} \mathbf{U}^{k,l} \mathbf{h}_u^l)) \quad (\text{S8})$$

Residual gated graph neural networks (gated GCN). The layer introduced in [5] embeds representations of nodes v (\mathbf{h}_v^l) and its edges ($\mathbf{e}_{u,v}^l, \forall u \in \mathcal{N}_v$) simultaneously with a residual mechanism. The edge embeddings e can also be used as *anisotropic* aggregating weights.

$$\mathbf{h}_v^{l+1} = \mathbf{h}_v^l + \text{ReLU}(\text{BN}(\mathbf{U}^l \mathbf{h}_v^l + \sum_{u \in \mathcal{N}_v} \mathbf{e}_{u,v}^l \otimes \mathbf{V}^l \mathbf{h}_u^l)) \quad (\text{S9})$$

$$\mathbf{e}_{u,v}^l = \frac{\sigma(\hat{\mathbf{e}}_{u,v}^l)}{\sum_{u \in \mathcal{N}_v} \sigma(\hat{\mathbf{e}}_{u,v}^l) + \epsilon} \quad (\text{S10})$$

$$\hat{\mathbf{e}}_{u,v}^l = \hat{\mathbf{e}}_{u,v}^{l-1} + \text{ReLU}(\text{BN}(\mathbf{A}^l \mathbf{h}_u^{l-1} + \mathbf{B}^l \mathbf{h}_v^{l-1} + \mathbf{C}^l \hat{\mathbf{e}}_{u,v}^{l-1})) \quad (\text{S11})$$

where $\text{BN}(\cdot)$ is batch normalization [12] and \otimes is element-wise multiplication. $\mathbf{U}^l \in \mathbb{R}^{D \times D}$, $\mathbf{V}^l \in \mathbb{R}^{D \times D}$, $\mathbf{A}^l \in \mathbb{R}^{D \times D}$, $\mathbf{B}^l \in \mathbb{R}^{D \times D}$, and $\mathbf{C}^l \in \mathbb{R}^{D \times D}$ are trainable parameters. We applied modular gradient weighting in Section 2.2 to the aggregating function of Equation S9 to define the *bi*-GatedGCN layer:

$$\mathbf{h}_v^{l+1} = \mathbf{h}_v^l + \text{ReLU}(\text{BN}(\mathbf{U}^l \mathbf{h}_v^l + \sum_{u \in \mathcal{N}_v} \mathbf{e}_{u,v}^l \otimes \hat{\beta}_{u,v}^l \mathbf{V}^l \mathbf{h}_u^l)) \quad (\text{S12})$$

B Results for the other configuration of the bilateral-GNN Network architecture

Figure S1 illustrates three configurations of network architecture using the *bilateral*-MP layer(s). A comparison of prediction performance across the configurations was performed using the gated GCN MP layer and ZINC dataset. As shown in Table S1, the *boosting* configuration achieved the best performance, while the other configurations were suboptimal.

C Benchmarking results for small-size dataset

Additionally, we demonstrated that the proposed *bilateral*-MP framework works well on several popular small datasets. We performed experiments on three TU graph classification datasets [24] with the same settings (data split, learning rate strategy, and batch size) as in [10]. A detailed description of the data statistics is provided in Table S2.

As shown in Table S3, the *bi*-GatedGCN and *bi*-GraphSAGE were consistently higher performing than the original MPs. In contrast, *bi*-GAT could not outperform the baseline GAT model. For the GCN, only the *bi*-GCN in the DD dataset exhibited a boost in prediction performance.

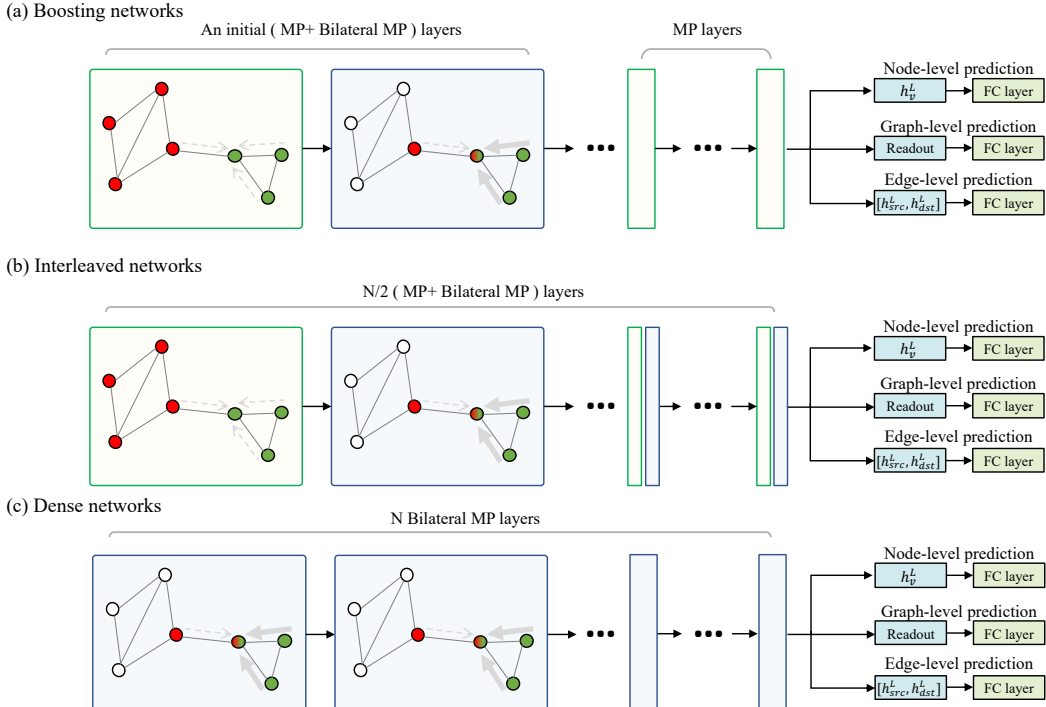


Figure S1: Three possible configurations of GNNs using the proposed bilateral MP layer(s).

Table S2: Statistics on three small benchmark datasets of TU. Columns 3 and 4 denote mean statistics for the number of nodes and edges, respectively. Columns 5 and 6 summarize the node and edge features (and dimension), respectively.

Dataset	#Graphs	#Nodes	#Edges	Node feat (dim)	Edge feat (dim)
DD	1178	284.32	715.66	Node labels (89)	—
ENZYMES	600	32.63	62.14	Node attributes (18)	—
PROTEINS	1113	39.06	72.82	Node attributes (29)	—

Table S3: Benchmarking results on four SOTA MP GNNs across datasets of small graph-level classification tasks. **Bold**: there are performance improvements with our *bilateral-MP* scheme. **Red**: Best performance.

DD											
Model	L	Params	Test ACC	Train ACC	Epochs	Model	L	Params	Test ACC	Train ACC	Epochs
GCN	4	102293	72.758 \pm 4.083	100.00 \pm 0.000	266.7	<i>bi</i> -GCN	4	117271	73.517 \pm 4.321	100.00 \pm 0.000	280
GraphSAGE	4	102577	73.433 \pm 3.429	100.00 \pm 0.000	267.2	<i>bi</i> -GraphSAGE	4	113435	74.193 \pm 2.482	100.00 \pm 0.000	267.2
GAT	4	100132	75.900 \pm 3.824	95.851 \pm 2.575	201.3	<i>bi</i> -GAT	4	117767	74.372 \pm 3.716	99.894 \pm 0.134	109.8
GatedGCN	4	104165	72.918 \pm 2.090	82.796 \pm 2.242	300.7	<i>bi</i> -GatedGCN	4	105227	73.862 \pm 3.069	94.014 \pm 2.088	237.2
ENZYMES											
Model	L	Params	Test ACC	Train ACC	Epochs	Model	L	Params	Test ACC	Train ACC	Epochs
GCN	4	103407	65.833 \pm 4.610	97.688 \pm 3.064	343	<i>bi</i> -GCN	4	113641	60.333 \pm 6.316	87.500 \pm 8.079	338.4
GraphSAGE	4	105595	65.000 \pm 4.944	100.00 \pm 0.000	294.2	<i>bi</i> -GraphSAGE	4	115033	68.333 \pm 2.687	100.00 \pm 0.000	303.1
GAT	4	101274	68.500 \pm 5.241	100.00 \pm 0.000	299.3	<i>bi</i> -GAT	4	104420	67.667 \pm 3.350	99.771 \pm 0.286	299.5
GatedGCN	4	103409	65.667 \pm 4.899	99.979 \pm 0.062	316.8	<i>bi</i> -GatedGCN	4	106237	68.167 \pm 5.747	100.00 \pm 0.000	322.2
PROTEINS											
Model	L	Params	Test ACC	Train ACC	Epochs	Model	L	Params	Test ACC	Train ACC	Epochs
GCN	4	104865	76.098 \pm 2.406	81.387 \pm 2.451	350.9	<i>bi</i> -GCN	4	116005	76.001 \pm 3.545	81.713 \pm 2.166	339
GraphSAGE	4	101928	75.289 \pm 2.419	85.827 \pm 0.839	245.4	<i>bi</i> -GraphSAGE	4	114199	76.996 \pm 2.933	87.704 \pm 1.522	242.6
GAT	4	102710	76.277 \pm 2.410	83.186 \pm 2.000	344.6	<i>bi</i> -GAT	4	110556	74.751 \pm 1.834	83.871 \pm 1.738	192.3
GatedGCN	4	104855	76.363 \pm 2.904	79.431 \pm 0.695	293.8	<i>bi</i> -GatedGCN	4	99830	76.453 \pm 3.109	79.858 \pm 0.449	337